Solid State Communications 147 (2008) 103–106

Contents lists available at ScienceDirect

Solid State Communications

journal homepage: www.elsevier.com/locate/ssc

# Specific heat and transport properties of $La_{1-x}Gd_xMnO_3$ at 15 K $\leq T \leq$ 300 K

Renu Choithrani [a,*], N.K. Gaur [a], R.K. Singh [a,b]

[a] Department of Physics, Barkatullah University, Bhopal (MP) – 462 026, India
[b] School of Basic Sciences, MATS University, Raipur (C.G.) – 492 002, India

ARTICLE INFO

*Article history:*
Received 9 February 2008
Received in revised form
25 April 2008
Accepted 2 May 2008 by
E.V. Sampathkumaran
Available online 13 May 2008

*PACS:*
75.47.Lx
74.25.Bt
75.80.+q

*Keywords:*
A. Manganites
A. CMR materials
D. Transport properties
D. Specific heat

ABSTRACT

We have investigated the specific heat and transport properties of the doped perovskite manganites $La_{1-x}Gd_xMnO_3$ with $0.0 \leq x \leq 1.0$ in the temperature range 15 K $\leq T \leq$ 300 K using the Modified Rigid Ion Model (MRIM), probably, for the first time. At room temperature, for all doping levels the orthorhombic 'O' phase is indicative of a strong Jahn–Teller distortion. Our theoretical results on the specific heat for $La_{1-x}Gd_xMnO_3$ ($x = 0.0$, 0.75 and 1.0) as a function of temperature 15 K $\leq T \leq$ 300 K are closer to the available experimental data with minor deviations at lower and higher temperatures. The MRIM results have predicted the observed anomalies for $x = 0.0$, 0.75, 1.0 in the temperature range 30 K $\leq T \leq$ 126 K and revealed new anomalies for $x = 0.25$ and 0.50 in the temperature range 50 K $\leq T \leq$ 100 K. Further, we have computed the temperature and composition ($x$) dependence of the transport properties, like the cohesive energy ($\phi$), Restrahalen frequency ($\upsilon_0$), Debye temperature ($\theta_D$) and Grüneisen parameter ($\gamma$) and compared them with the experimental data available only at room temperature (300 K) for the concentrations $x = 0.0$ and 1.0.



## 1. Introduction

The doped perovskite manganites like $La_{1-x}Gd_xMnO_3$ $0.0 \leq x \leq 1.0$ [1] have attracted unprecedented attention due to the occurrence of colossal magnetoresistance (CMR) effects [2] and their technological potential. The Gd doped $LaMnO_3$ have a very rich phase diagram, depending on the doping concentration, temperature and pressure, being either an anti-ferromagnetic insulator, ferromagnetic metal or charge-ordered insulators. These interesting phenomena pose the necessity of understanding the mechanism behind their origin and the thermodynamic and transport properties of doped manganites.

The crystal structure of $LaMnO_3$ (space group *pnma*) has an orthorhombic structure with four formula units per unit cell. The occurrence of spin and orbital ordered state in them has been understood in terms of the cooperative Jahn–Teller distortion [3].

In this communication, we have predicted the specific heat and transport properties of $La_{1-x}Gd_xMnO_3$ ($0.0 \leq x \leq 1.0$) as a function of temperature 15 K $\leq T \leq$ 300 K using the Modified Rigid Ion Model [4], probably, for the first time. The formalism of the model is described in Section 2 and the results of its application are presented and discussed in Section 3.

## 2. Essential formalism of modified RIM

We have modified the framework of rigid ion model (RIM) [4] by including the effects of short-range (SR) Hafemeister–Flygare (HF) type [5] overlap repulsion operative upto the second neighbour ions and van der Waals (vdW) attraction due to dipole–dipole (d–d) and dipole–quadrupole (d–q) interactions [6]. The total potential of the Modified RIM (MRIM) is expressed as

$$\phi = -\frac{e^2}{2}\sum_{kk'} Z_k Z_{k'} r_{kk'}^{-1} + nb_1\beta_{kk'}\exp\{(r_k + r_{k'} - r_{kk'})/\rho_1\} + \frac{n'}{2}b_2[\beta_{kk}\exp\{(2r_k - r_{kk})/\rho_2\} + \beta_{k'k'} \times \exp\{(2r_{k'} - r_{k'k'})/\rho_2\}] - \sum_{kk'} c_{kk'} r_{kk'}^{-6} - \sum_{kk'} d_{kk'} r_{kk'}^{-8}. \quad (1)$$

Here, $k$ ($k'$) denotes the positive (negative) ions and the sum is taken over all ($kk'$) ions. $\beta_{kk'}$ are the Pauling coefficients

$$\beta_{kk'} = 1 + (z_k/n_k) + (z_{k'}/n_{k'}) \quad (2)$$

with $z_k(z_{k'})$ and $n_k$ ($n_{k'}$) as the valence and number of electrons in the outermost orbits of $k$ ($k'$) ions and $r_{kk'}$ and $r_{kk}(= r_{k'k'})$ are the first and second neighbour separations, respectively. In Eq. (1), the first term represents the long-range (LR) Coulomb attraction, the second and third terms are SR HF type repulsion [5] between

* Corresponding author. Tel.: +91 755 2745677; fax: +91 755 2677723.
*E-mail address:* renuchoithrani@gmail.com (R. Choithrani).

0038-1098/$ – see front matter © 2008 Elsevier Ltd. All rights reserved.
doi:10.1016/j.ssc.2008.05.005

**Table 1**
Model parameters and transport properties of $La_{1-x}Gd_xMnO_3$

| Conc. ($x$) | Temp (K) | Model parameters | | | | Transport properties | | | |
|---|---|---|---|---|---|---|---|---|---|
| | | Mn–O $\rho_1$ (Å) | Mn–O $b_1(10^{-12}$ erg) | La/Gd–O $\rho_2$ (Å) | La/Gd–O $b_2(10^{-12}$ erg) | $\phi$ (eV) | $\upsilon_0$ (THz) | $\Theta_D$ (K) | $\gamma$ |
| | 15 | 0.4760 | 0.9926 | 0.6411 | 1.5648 | −141.81 | 8.899 | 426.939 | 2.231 |
| | 65 | 0.4751 | 0.9879 | 0.6400 | 1.5615 | −141.85 | 8.917 | 427.763 | 2.238 |
| | 115 | 0.4742 | 0.9831 | 0.6388 | 1.5582 | −141.89 | 8.935 | 428.584 | 2.245 |
| | 165 | 0.4733 | 0.9784 | 0.6377 | 1.5549 | −141.94 | 8.942 | 429.403 | 2.252 |
| **0** | 215 | 0.4724 | 0.9737 | 0.6365 | 1.5516 | −141.98 | 8.967 | 430.219 | 2.259 |
| | 265 | 0.4715 | 0.9691 | 0.6354 | 1.5483 | −142.02 | 8.984 | 431.033 | 2.266 |
| | | | | | | −142.05 | 8.990 | 431.601 | 2.271 |
| | 300 | 0.4709 | 0.9658 | 0.6346 | 1.5460 | (−141.81)[a] | (8.58)[b] | (388)[c] | (2–3)[d] |
| | 15 | 0.5102 | 1.1766 | 0.6819 | 1.6952 | −143.00 | 9.021 | 434.343 | 2.372 |
| | 65 | 0.5093 | 1.1714 | 0.6807 | 1.6917 | −143.05 | 9.103 | 435.252 | 2.374 |
| | 115 | 0.5083 | 1.1662 | 0.6795 | 1.6882 | −143.10 | 9.125 | 435.158 | 2.376 |
| **0.25** | 165 | 0.5074 | 1.1611 | 0.6783 | 1.6847 | −143.15 | 9.141 | 436.176 | 2.378 |
| | 215 | 0.5065 | 1.1560 | 0.6771 | 1.6812 | −143.21 | 9.164 | 438.661 | 2.380 |
| | 265 | 0.5055 | 1.1509 | 0.6759 | 1.6777 | −143.26 | 9.182 | 438.858 | 2.382 |
| | 300 | 0.5049 | 1.1473 | 0.6750 | 1.6753 | −143.29 | 9.194 | 439.485 | 2.384 |
| | 15 | 0.5467 | 1.3800 | 0.7292 | 1.8305 | −144.91 | 9.201 | 440.282 | 2.440 |
| | 65 | 0.5457 | 1.3744 | 0.7279 | 1.8268 | −144.97 | 9.214 | 441.290 | 2.446 |
| | 115 | 0.5447 | 1.3689 | 0.7267 | 1.8231 | −144.03 | 9.223 | 442.294 | 2.449 |
| **0.50** | 165 | 0.5437 | 1.3633 | 0.7255 | 1.8194 | −144.09 | 9.245 | 443.295 | 2.456 |
| | 215 | 0.5427 | 1.3578 | 0.7242 | 1.8157 | −144.15 | 9.264 | 444.293 | 2.458 |
| | 265 | 0.5418 | 1.3522 | 0.7230 | 1.8120 | −144.21 | 9.281 | 445.287 | 2.464 |
| | 300 | 0.5411 | 1.3484 | 0.7221 | 1.8094 | −144.25 | 9.291 | 447.981 | 2.468 |
| | 15 | 0.5854 | 1.6030 | 0.7792 | 1.9761 | −145.45 | 9.301 | 450.192 | 2.521 |
| | 65 | 0.5844 | 1.5970 | 0.7779 | 1.9722 | −145.52 | 9.310 | 450.829 | 2.526 |
| | 115 | 0.5834 | 1.5911 | 0.7766 | 1.9683 | −145.59 | 9.321 | 450.962 | 2.530 |
| **0.75** | 165 | 0.5823 | 1.5851 | 0.7753 | 1.9644 | −145.65 | 9.328 | 450.981 | 2.536 |
| | 215 | 0.5813 | 1.5792 | 0.7740 | 1.9605 | −145.72 | 9.331 | 450.988 | 2.540 |
| | 265 | 0.5803 | 1.5733 | 0.7727 | 1.9566 | −145.79 | 9.337 | 450.998 | 2.544 |
| | 300 | 0.5796 | 1.5691 | 0.7718 | 1.9539 | −145.84 | 9.339 | 451.315 | 2.548 |
| | 15 | 0.6326 | 1.8838 | 0.8397 | 2.1573 | −146.717 | 9.492 | 455.569 | 2.676 |
| | 65 | 0.6318 | 1.8774 | 0.8383 | 2.1532 | −146.765 | 9.509 | 456.375 | 2.686 |
| | 115 | 0.6307 | 1.8710 | 0.8370 | 2.1490 | −146.813 | 9.525 | 457.160 | 2.697 |
| | 165 | 0.6296 | 1.8646 | 0.8357 | 2.1449 | −146.861 | 9.541 | 457.943 | 2.707 |
| **1.0** | 215 | 0.6286 | 1.8582 | 0.8343 | 2.1407 | −146.908 | 9.558 | 458.725 | 2.718 |
| | 265 | 0.6274 | 1.8519 | 0.8330 | 2.1366 | −146.956 | 9.574 | 459.506 | 2.728 |
| | | | | | | | | 460.051 | 2.735 |
| | 300 | 0.6267 | 1.8474 | 0.8321 | 2.1337 | −146.989 | 9.589 | (474)[e] | (2–3)[d] |

[a] Ref. [17].
[b] Ref. [18].
[c] Ref. [19].
[d] Ref. [20].
[e] Refs. [1,9].

the first and second neighbour ions, respectively. The last two terms are vdW attraction due to d–d and d–q interactions. $c_{kk'}$ and $d_{kk'}$ are the vdW coefficients whose values are determined from the following expressions derived from the Slater–Kirkwood variational method [7]:

$$c_{kk'} = (3e\hbar\alpha_k\alpha_{k'}/2m)[(\alpha_{k/N_k})^{1/2} + (\alpha_{k'/N_{k'}})^{1/2}]^{-1} \quad (3)$$

$$d_{kk'} = (27e\hbar^2\alpha_k\alpha_{k'}/8m)[(\alpha_{k/N_k})^{1/2} + (\alpha_{k'/N_{k'}})^{1/2}]^2 \times [(\alpha_{k/N_k})^{1/2} + 20/3(\alpha_k\alpha_{k'/N_kN_{k'}})(\alpha_{k'/N_{k'}})]^{-1} \quad (4)$$

where $m$ and $e$ are the mass and charge of the electrons, respectively. $\alpha_k(\alpha_{k'})$ are the polarizabilities of $k(k')$ ions; $N_k(N_{k'})$ are the effective number of electrons responsible for the polarization of $k(k')$ ions.

The model parameters (hardness ($b$) and range ($\rho$)) are determined from the equilibrium condition:

$$[d\phi(r)/dr]_{r=r_0} = 0 \quad (5)$$

and the isothermal bulk modulus:

$$B_T = (9Kr_0)^{-1}[d^2\phi(r)/dr^2]_{r=r_0}. \quad (6)$$

Here, $K$ is the crystal structure constant and $r_o$ is the equilibrium interionic separation.

The calculated values of the model parameters ($b_1$, $\rho_1$) and ($b_2$, $\rho_2$) are depicted in Table 1 for Mn–O and La/Gd–O bonds, respectively.

The specific heat of $La_{1-x}Gd_xMnO_3$ is calculated at different temperatures ($T$) and concentrations ($x$) using the well-known expression [7]:

$$C_V = 9R\left(\frac{T}{\theta_D}\right)^3 \int_0^{\frac{\theta_D}{T}} \frac{e^x x^4}{e^x - 1} dx. \quad (7)$$

Besides, we have computed the cohesive energy ($\phi$), Restrahalen frequency ($\upsilon_0$), Debye temperature ($\theta_D$) and Grüneisen parameter ($\gamma$) of $La_{1-x}Gd_xMnO_3$ using their expressions reported in our earlier papers [6] and the model parameters listed in Table 1. The computed results are presented and discussed below.

## 3. Results and discussion

The values of input data ($r_0$, $B_T$) for the evaluation of model parameters ($b_1$, $\rho_1$ and $b_2$, $\rho_2$) corresponding to Mn–O and La/Gd–O bonds at different compositions ($x$) and temperatures ($T$) are obtained from the well-known Vegard's law using their experimental data [1,8–16] of the end point materials $LaMnO_3$ and

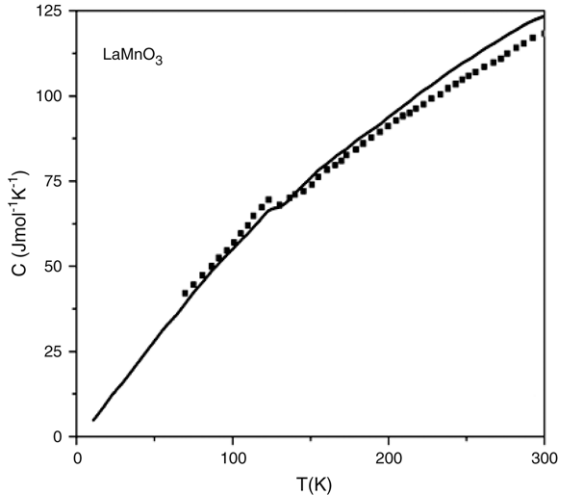


**Fig. 1.** The specific heat of $LaMnO_3$, where the solid line (—) and the squares (■) are the present theoretical and experimental [21] results, respectively.

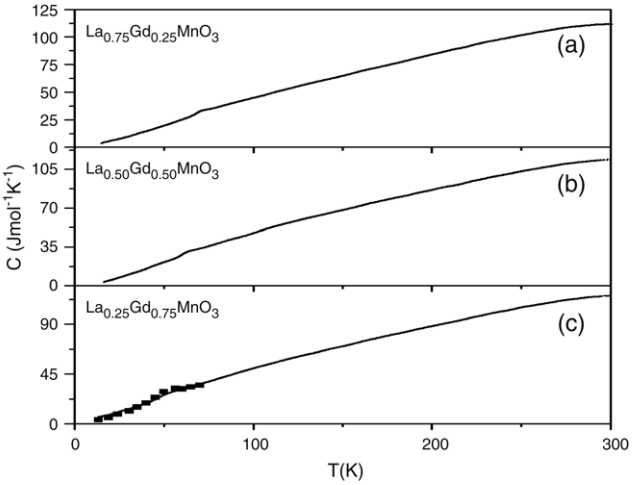


**Fig. 2.** ((a), (b), (c)). The specific heat of $La_{0.75}Gd_{0.25}MnO_3$, $La_{0.50}Gd_{0.50}MnO_3$ and $La_{0.25}Gd_{0.75}MnO_3$, where the solid lines (—) and the squares (■) are the present theoretical and experimental [1] results, respectively.

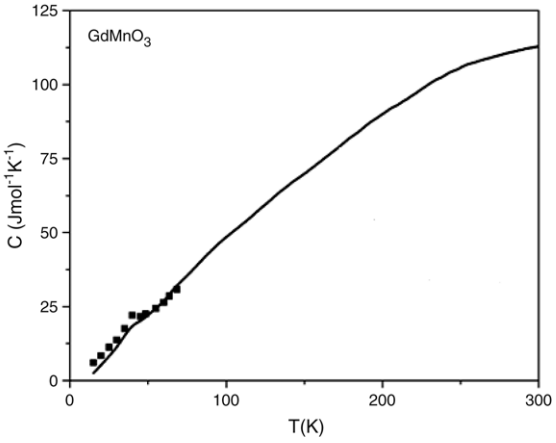


**Fig. 3.** The specific heat of $GdMnO_3$, where the solid line (—) and the squares (■) are the present theoretical and experimental [1] results, respectively.

$GdMnO_3$. Using these input data and vdW coefficients evaluated for $La_{1-x}Gd_xMnO_3$, we have computed the model parameters ($b_1$, $\rho_1$; $b_2$, $\rho_2$) using Eqs. (5) and (6) for different compositions ($x = 0.0, 0.25, 0.50, 0.75$ and $1.0$) and temperatures ($15\ K \leq T \leq 300\ K$) and listed them in Table 1.

Using the values of these model parameters, we have computed the cohesive energy ($\phi$) for $La_{1-x}Gd_xMnO_3$ ($0.0 \leq x \leq 1.0$). It is seen from Table 1 that the magnitude of the cohesive energy increases systematically from $\phi = -142.05$ eV for $x = 0.0$ (i.e. $LaMnO_3$) to $-146.989$ eV for $x = 1.0$ (i.e. $GdMnO_3$). Also, our values of the cohesive energy for pure $LaMnO_3$ ($x = 0.0$) is in good agreement with the experimental data [17] available only for $x = 0.0$ at room temperature. The negative values of cohesive energy show that the stability of the compound is intact. The values of Restrahalen frequency ($\upsilon_0$) (see Table 1) are increasing with Gd concentration ($x$) and temperature ($T$), which shows that the bond is becoming stronger with Gd doping. The hardness ($b_1$, $b_2$) and the stability ($-\phi$) of the material are also increasing with the increase of $x$. Our calculated Restrahlen frequency (8.99 THz) for $LaMnO_3$ ($x = 0.0$) are closer to the experimental data (8.58 THz) [18] available only at 300 K.

The calculated values of Debye temperature ($\theta_D$) for $LaMnO_3$ (at $x = 0.0$) and $GdMnO_3$ (at $x = 1.0$) are almost in good agreement with their corresponding experimental data ($\theta_D = 388$ K) for $LaMnO_3$ and ($\theta_D = 474$ K) [1,9,19] for $GdMnO_3$ available only at 300 K. The higher values of Debye temperature indicate the presence of higher phonon frequencies in these manganites. The calculated values of Debye temperature of $La_{1-x}Gd_xMnO_3$ (for $x = 0.0$–$1.0$) at temperature $15\ K \leq T \leq 300$ K are 426.93–460.05 K, which seems within the range of Debye temperature (300–550 K) often found in perovskite manganites. Our calculated Grüneisen parameters ($\gamma$) are increasing with composition (x) from 0 to 1.0 and temperature range $15\ K \leq T \leq 300$ K and its values lie in between 2 and 3 as reported by Dia et al. [20].

The specific heat (C) values calculated for $La_{1-x}Gd_xMnO_3$ in the temperature range $15\ K \leq T \leq 300$ K for Gd concentrations $0.0 \leq x \leq 1.0$ are displayed in Figs. 1–3 and compared with the available experimental data [1,21]. It is noticed from Fig. 1 that temperature variations of calculated specific heat for undoped $LaMnO_3$ is almost in fair agreement with the experimental data [21] in the temperature range $50\ K \leq T \leq 125$ K. Such a close match between theoretical and experimental [21] results are remarkable in a $LaMnO_3$ system which shows the orbital, lattice, magnetic and strong correlation effects. The deviations at higher temperature range $150\ K \leq T \leq 300$ K might be due to the exclusion of anharmonic effects in the MRIM framework. The Fig. 1 also depicts that the undoped $LaMnO_3$ undergoes the transition from paramagnetic to ferromagnetic state at 126 K as is indicated by a peak in the specific heat curve. This feature is revealed from both the present theoretical and experimental [21] results. On Gd doping (for $x = 0.25$, 0.50 and 0.75) in $LaMnO_3$, the specific heat increases systematically with temperature as is seen from Fig. 2((a), (b), (c)). Our theoretical results on the specific heat for $La_{0.75}Gd_{0.25}MnO_3$, $La_{0.50}Gd_{0.50}MnO_3$ and $La_{0.25}Gd_{0.75}MnO_3$ have shown an anomaly around 60–70 K (see Fig. 2((a), (b), (c)) which might be the similar magnetic transitions as exhibited by the undoped $LaMnO_3$ ($x = 0.0$) and $GdMnO_3$ ($x = 1.0$) compounds (see Figs. 1 and 3).

It is seen from Figs. 2(c) and 3 that a cusp-like anomaly occurs at 40–60 K. These features correspond to the transition from paramagnetic to canted antiferromagnetic (CA) state. A shoulder is displayed in Figs. 2(c) and 3 by the specific heat (C) curve below $T_{CA}$ and the sharp increase towards the low temperatures exhibited by both the theoretical and experimental [1] results reveal the polarization of Gd spins within the effective field of Mn sublattice, but no evidence for a further magnetic transition of Mn sublattice into an incommensurate phase was found. It is interesting to note from Figs. 2(c) and 3 that our specific heat results are almost in good agreement with the experimental data [1] in the range $25\ K \leq T \leq 75$ K, but they show remarkable deviations at lower

temperatures 0 K $\leq T \leq$ 25 K in both the manganites. These deviations might be partly due to the exclusion of the effects of zero-point energy and the change in entropy in the framework of the MRIM. Our results on the specific heat at $x = 0.25$ and 0.50 could not be compared due to the lack of experimental data, hence they will serve as a guide to the experimental workers in future.

## 4. Conclusion

On the basis of the overall discussions it may be concluded that the specific heats (Figs. 1–3) at lower and higher temperatures show a significant change and many interesting features. The slight deviations in the specific heat values (Figs. 1–3) between the low and high temperatures are, probably, due to the dominant role played by the Jahn–Teller (JT) effect in $La_{1-x}Gd_xMnO_3$ in this temperature range. Here, it is noteworthy that a quantitative estimate of the JT effect would make the results of study more useful. It is also interesting to note that our results on temperature dependence of specific heat have revealed an anomaly at lower temperatures for all the compositions ($x$). These anomalies have shifted to the lower temperatures with increasing Gd doping for $0.0 \leq x \leq 1.0$. This might be due to the strong Jahn–Teller distortion at lower temperatures.

The description of the specific heat and transport properties for $La_{1-x}Gd_xMnO_3$ system seems remarkable in view of the inherent simplicity of the Modified Rigid Ion Model. Our theoretical results on these properties at lower and higher temperatures can be improved further by incorporating the effects of ferromagnetic spin wave contributions, zero-point energy, change in entropy and anharmonicity in the framework of the MRIM

## Acknowledgements

The authors are thankful to the University Grants Commission (UGC), New Delhi for providing the financial support. One of us (Renu Choithrani) is also thankful to the Council of Scientific and Industrial Research for the award of Senior Research Fellowship.

## References

[1] J. Hemberger, S. Lobina, H-A. Krug Von Nidda, N. Tristan, V.Yu. Ivanov, A.A. Mukhin, A.M. Balbashov, A. Loidl, Phys. Rev. B 70 (2004) 024414.
[2] R.Von. Helmolt, J. Weeker, B. Holzapfel, L. Schultz, K. Samwer, Phys. Rev. Lett. 71 (1993) 233.
[3] B. Dabrowski, S. Kolesnik, A. Baszczuk, O. Chmaissen, T. Maxwell, J. Mais, J. Solid State Chem. 178 (2005) 629.
[4] R.K. Singh, Phys. Rep. (Netherland) 85 (1982) 259.
[5] D.W. Hafemiester, W.H. Flygare, J. Chem. Phys. 43 (1965) 795.
[6] Renu Choithrani, N.K. Gaur, J. Magn. Magn. Mater. 320 (2008) 612; Solid State Commun. 145 (2008) 308.
[7] J.C. Slater, K.G. Kirkwood, Phys. Rev. Lett. 37 (1931) 682.
[8] J. Baier, D. Meier, K. Berggold, J. Hemberger, A. Balbashov, J.A. Mydosh, T. Lorenz, J. Magn. Magn. Mater. 310 (2007) 1165–1167 and references there in.
[9] T. Kimura, S. Ishihara, H. Shintani, T. Arima, K.T. Takahashi, K. Ishizaka, Y. Tokura, Phys. Rev. B 68 (2003) 060403.
[10] J. Baier, D. Meir, K. Berggold, J. Hemberger, A. Balbashov, J.A. Mydosh, T. Lorenz, Phys. Rev. B 73 (2006) 100402 (R).
[11] T. Arima, T. Goto, Y. Yamasaki, S. Miyasaka, K. Ishii, M. Tsubota, T. Inami, Y. Murakami, Y. Tokura, arXiv:cond-mat/ 0508580 V1, 24 Aug. 2005.
[12] M.N. Iliev, M.V. Abrashev, J. Laverdiere, S. Jandl, M.M. Gospodinov, Y.-Q. Wang, Y.-Y. Sun, Phys. Rev. B 73 (2006) 064302.
[13] J. Laverdier, S. Jandl, A.A. Mukhin, V.Yu. Ivanov, V.G. Ivanov, M.N. Iliev, Phys. Rev. B 73 (2006) 214301.
[14] T. Arima, T. Goto, Y. Yamasaki, S. Miyasaka, K. Ishii, M. Tsubota, T. Inami, Y. Murakami, Y. Tokura, Phys. Rev. B 72 (2005) 100102 (R).
[15] T. Kimura, G. Lawes, T. Goto, Y. Tokura, A.P. Ramirez, Phys. Rev. B 71 (2005) 224425.
[16] M.W. Kim, S.J. Moon, J.H. Jung, Jaejun Yu, Sachin Parashar, P. Murugavel, J.H. Lee, T.W. Noh, Phys. Rev. Lett. 96 (2006) 247205.
[17] Roger A. De Souza, M. Saiful Islam, Ellen Ivers-Tiffe, J. Mater. Chem. 9 (1999) 1621;
N.N. Kovalova, J.L. Gavartin, A.L. Shluger, A.M. Stoneham, Physica B 734 (2002) 312.
[18] I. Fedorov, J. Lorenzana, P. Dore, G.De. Marzi, P. Maselli, P. Calvani, S-W. Cheong, S. Koval, R. Migoni, Phys. Rev. B 60 (1999) 11875.
[19] P.G. Radaelli, S-W. Cheong, Phys. Rev. B 66 (2002) 094408.
[20] P. Dai, Zhang Jiandi, H.A. Mook, S.H. Lion, P.A. Dowben, E.W. Plummer, Phys. Rev. B 54 (1996) 3694(R).
[21] A. Michalopoulou, C. Papastaicoudis, E. Syskakis, Physica B 284 (2000) 1412.